Optics and Lasers in Engineering ■ (■■■■) ■■■–■■■

Contents lists available at ScienceDirect

Optics and Lasers in Engineering

journal homepage: www.elsevier.com/locate/optlaseng

Substrate-dependent cell elasticity measured by optical tweezers indentation

Muhammad S. Yousafzai [a,b], Fatou Ndoye [c,d], Giovanna Coceano [a,b], Joseph Niemela [c], Serena Bonin [e], Giacinto Scoles [f], Dan Cojoc [a,*]

[a] Institute of Materials (IOM-CNR), Area Science Park, Basovizza, S.S. 14, Km 163.5, 34149 Trieste, Italy
[b] Nanotechnology, University of Trieste, 34149 Trieste, Italy
[c] International Centre for Theoretical Physics (ICTP), 34149 Trieste, Italy
[d] Department of Physics, Cheikh Anta Diop University, Dakar 5005, Senegal
[e] Department of Medical Sciences (DSM), University of Trieste, 34149, Italy
[f] Department of Biological and Medical Science, University of Udine, Santa Maria della Misericordia Hospital, 33100 Udine, Italy

ARTICLE INFO

Article history:
Received 5 November 2014
Received in revised form
16 February 2015
Accepted 22 February 2015

Keywords:
Cell elasticity
Biomechanics
Optical tweezers
Elastic modulus
Substrate stiffness

ABSTRACT

In the last decade, cell elasticity has been widely investigated as a potential label free indicator for cellular alteration in different diseases, cancer included. Cell elasticity can be locally measured by pulling membrane tethers, stretching or indenting the cell using optical tweezers. In this paper, we propose a simple approach to perform cell indentation at pN forces by axially moving the cell against a trapped microbead. The elastic modulus is calculated using the Hertz-model. Besides the axial component, the setup also allows us to examine the lateral cell–bead interaction. This technique has been applied to measure the local elasticity of HBL-100 cells, an immortalized human cell line, originally derived from the milk of a woman with no evidence of breast cancer lesions. In addition, we have studied the influence of substrate stiffness on cell elasticity by performing experiments on cells cultured on two substrates, bare and collagen-coated, having different stiffness. The mean value of the cell elastic modulus measured during indentation was 26 ± 9 Pa for the bare substrate, while for the collagen-coated substrate it diminished to 19 ± 7 Pa. The same trend was obtained for the elastic modulus measured during the retraction of the cell: 23 ± 10 Pa and 13 ± 7 Pa, respectively. These results show the cells adapt their stiffness to that of the substrate and demonstrate the potential of this setup for low-force probing of modifications to cell mechanics induced by the surrounding environment (e.g. extracellular matrix or other cells).

1. Introduction

The pioneering work by Ashkin et. al. on the trapping of micro-particles and their manipulation by radiation pressure [1,2] led to the foundation of a new tool called optical tweezers (OT), which has found a multitude of applications in physics, chemistry and biology [3–5]. An important achievement for biology was the first demonstration that living micro-organisms (e.g. viruses, bacteria) could be manipulated by OT without being damaged [6]. This was followed by trapping and manipulation of single cells [7] and cell-organelles [8] using infrared (IR) laser beams.

Although the levels of intensity were high (typically tens of MW/cm^2, roughly corresponding to focusing 100 mW beams on an area of about 1 μm^2), the use of IR laser beams proved to be non-damaging to cells. Another important achievement was the measurement of the forces generated by organelle transport in vivo [9] and the use of a trapped microbead to probe forces in single-cell and single-molecule experiments [10–12]. OT versatility is highlighted by the wide range of applications which this technique has enabled: OT are now being used in the investigation of an increasing number of biochemical and biophysical processes, from the basic mechanical properties of biological polymers to the multitude of molecular machines that drive the internal dynamics of the cell [13]. Since OT forces are in the range from 1 to 200 pN and trap stiffness is in the range 0.001–1 pN/nm, it represents a complementary tool to other techniques for manipulation and force probing, such as atomic force microscopy (AFM) or magnetic tweezers [14,15].

Cellular processes as motility, adhesion, cell division and proliferation, involve mechanical forces in the range of the above-mentioned techniques, making them ideal tools for investigating the mechanisms of such processes. There is a continuous biomechanical interaction

* Corresponding author.
E-mail address: cojoc@iom.cnr.it (D. Cojoc).

http://dx.doi.org/10.1016/j.optlaseng.2015.02.008
0143-8166/

between the cells and their extracellular matrix (ECM), and with other cells, leading to the modification of the cell biomechanics [16–18]. Moreover, the hypothesis that cellular biomechanics may play a significant role in tumorigenesis, cancer invasion and metastasis gains more and more support [19–21], although it is not yet fully understood how the transformation from healthy to malignancy alters the mechanical properties within the tumor microenvironment [22,23]. Among the various properties of cell mechanics, viscoelasticity has been the most widely investigated, e.g., using membrane tether pulling, cell stretching and indentation, all of which can be implemented in AFM and OT setups [24–27]. AFM applies higher forces to the sample than does OT (tens of pN compared to tens of nN) and the probe is stiffer (cantilever stiffness > 10 pN/nm). Since the response of the cell to mechanical stress depends on the applied force and the stiffness of the probe, these parameters need to be taken into account when interpreting measurements. Moreover, since the mechanical properties of biological samples depend on the loading rate (measured in N/s), quantifying the viscoelastic properties of a cell makes little sense without also defining the loading rate at which this property was measured [28,29]. In fact, the combination of both techniques allows the investigation of single cells at small and large forces and/or loading rates, enabling a more complete characterization of cell mechanics. A first comparative study of cell elasticity measurements by vertical indentation using AFM and OT was reported for 3T3 fibroblasts [30]. For comparable loading rates, indeed, the elastic modulus determined by OT is much smaller than that calculated by AFM. So far, AFM has been more frequently applied to cell elasticity measurement, due to the faster development of this technology for cell biology. However, the lowest force that can be reliably controlled in AFM is of the order of tens of pN, and these forces can already lead to a strain large enough to enter the non-elastic deformation regime [18]. Therefore OT, can provide in many cases a more appropriate and useful tool for a detailed understanding the properties of the cellular composite material. Another implementation of axial cell indentation using an OT setup was recently reported for the measurement of localized cell stiffness of Balb3T3 cells [31]. In both OT implementations [30,31] a trapped microbead is axially pushed against the cell by moving the trap, and cell indentation is determined by measuring the axial displacement of the bead.

In this paper, we propose an alternative OT approach to perform cell indentation at pN forces by axially moving the cell against the trapped microbead and measuring its displacement. Since the position of the trap is fixed, the displacement of the microbead directly reflects its interaction with the cell, avoiding possible interference with drifts during trap axial displacement. Therefore, this solution is conceptually more precise than the trap displacement solution used in previously mentioned works [30,31]. The optical setup and the measurement approach are presented in Section 2. The technique has been applied to measure the elastic modulus of HBL-100 cells. HBL-100 has already been used as a non-neoplastic model when studying the properties of breast cancer cell lines, such as MCF-7 or MDA-MB-231, but it has not been characterized from the mechanical point of view. Cell preparation is described in Section 3. In Section 4 we report measured cell elasticity for cells cultured on two different substrates: bare and collagen coated glass cover slips, and demonstrate the adaptability of cells to the substrate stiffness (knowing that cells sense their mechanical environment and change their response accordingly).

2. Apparatus and protocol for OT cell indentation

2.1. Optical tweezers setup

A modular Thorlabs optical tweezers kit [32] with some modifications has been used in this work. We also performed multiple trapping experiments with this setup (using dynamic arrays of traps generated by diffractive optical elements [33]) and for that reason we replaced the original laser trapping source (single mode laser diode, 975 nm, max 300 mW) by a more powerful IR laser (single mode Yb fiber laser YLM-5, 1064 nm, max 5 W, IPG Photonics GmbH), as shown in Fig. 1. The laser head has a built-in collimator providing a TEM00 laser beam with a diameter $D=5$ mm. After reflection by mirror M1 (which helps for alignment) the beam passes through a 2X beam expander, increasing its diameter to slightly overfill the entrance pupil of the microscope lens (Nikon 100X, NA 1.25 oil immersion, WD 0.3). The laser beam is focused into the sample chamber by the microscope lens, where a silica microbead is trapped at the point of focus. A home-made temperature controlled holder [24] is connected to the sample chamber (a Petri dish) to keep the cells at the physiological temperature, $T=37\ ^{\circ}C$ during the experiments. This is mounted on a nano-piezo cube, PS, (Thorlabs, NanoMax 3-axis flexure stage) allowing 5 nm control of the sample displacement. A second microscope lens (Nikon 10X, NA 0.25, WD 7) collects the laser light scattered by the trapped bead. The scattered light interferes in the back focal plane (BFP) of the second lens. The interference pattern (IP) is imaged by lens L3 ($f=40$ mm) onto the quadrant photo detector, QPD, (Thorlabs, PDQ80A, detector size 7.8 mm) which senses the lateral and axial displacement of the trapped bead, as indicated. When the bead is in the equilibrium position, the IP is centered on the QPD. A lateral displacement of the bead is indicated by an IP lateral displacement, while an axial displacement is indicated by the change in size of the IP. The lateral and axial differential signals (ΔX, ΔY, ΔZ) are obtained combining the signals from the quadrants 1–4 as follows:

$$\Delta X=[(1+4)-(2+3)]\ ;\ \Delta Y=[(1+2)-(3+4)]\ ;\ \Delta Z=[1+2+3+4] \tag{1}$$

The differential signals are acquired through a digital acquisition card (DAQ – NI USB 2561) and a custom LabView code running on a PC. As the QPD has a large bandwidth (150 kHz), it can measure very well the thermal movement of the bead in the trap, characterized by a maximum bandwidth of 1–2 kHz. The sample is illuminated by the light from a LED through the second microscope lens. The sample is imaged by the first microscope lens and the tube lens (TL) on the sensor of a CMOS camera (Thorlabs, DCC 1240C).

2.2. Experimental procedure.

Cell indentation is observed by moving axially the cell against the trapped bead, as shown in Fig. 2. When contact is made, the bead will try to resist cell advancement, producing an indentation of the cell. As the stage displacement (SD) is known and bead displacement (BD) can be measured by BFP interferometry as previously shown, it is possible to measure the bead movement into the cells, i.e. the indentation, Id:

$$Id = SD - BD \tag{2}$$

Another parameter required to calculate the elasticity is the force, F, exerted by the cell on the bead. This is given by the linear relation:

$$F = k \cdot BD \tag{3}$$

where k is the stiffness of the optical trap. This linear relation for the force is valid for a limited range of BD (± 500 nm) [14].

At the beginning of each single cell experiment, a bead is trapped and a cell is positioned slightly below it, preventing cell–bead contact. The microscope image of a HBL-100 cell under a trapped bead is shown in Fig. 2c. The PS is then vertically displaced with a sinusoid signal (amplitude $A=1.14$ μm, one period $T=5$ s) as shown in Fig. 3, and the vertical displacement of the bead in the trap is acquired at a 10 KHz sampling frequency (dark blue curve).

Please cite this article as: Yousafzai MS, et al. Substrate-dependent cell elasticity measured by optical tweezers indentation. Opt Laser Eng (2015), http://dx.doi.org/10.1016/j.optlaseng.2015.02.008

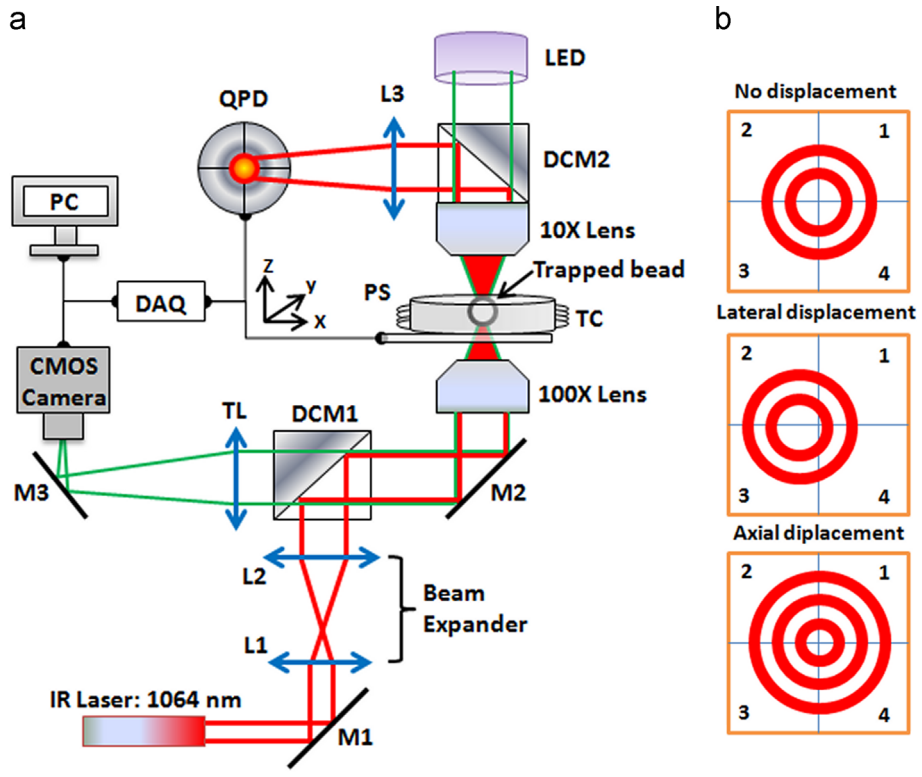

Fig. 1. Optical tweezers setup for cell indentation and force measurement. (**a**) Laser trapping (1064 nm) beam path (red) and bright-field imaging path (green). PS: 3-axis nano-piezo stage; DAQ: digital analog acquisition card; TL: tube lens; L1–L3 convergent lenses; M1–M3: mirrors; DCM 1–2 dichroic mirrors, TC: temperature controlled holder and (**b**) interference pattern imaged on the QPD for: equilibrium position, lateral and axial displacements. (For interpretation of the references to colour in this figure legend, the reader is referred to the web version of this article).

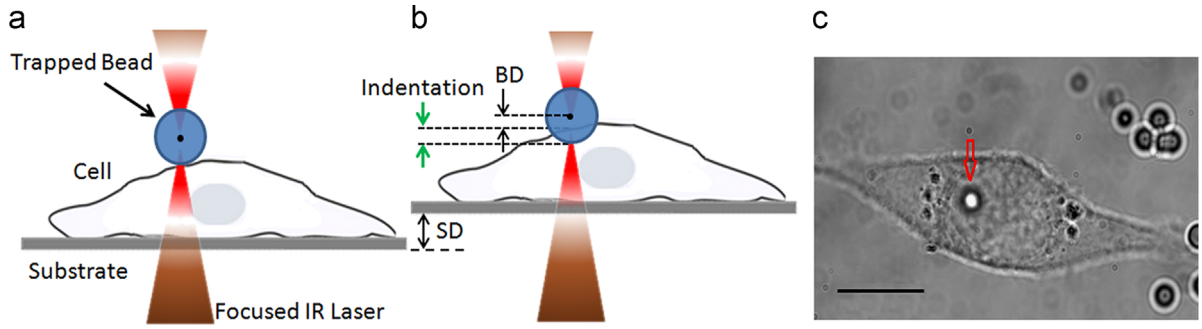

Fig. 2. Schematic of the experimental procedure. (**a**) The cell is positioned below the trapped bead, (**b**) the stage is moved up by *SD* and the cell interacts with the bead displacing it by *BD*, while the bead indents the cell and (**c**) optical microscope image of the bead above the cell, bead indicated by arrow, scale bar 10 μm.

During the first half of the period, the PS moves away from the bead, therefore the bead oscillates freely in the trap. This signal can be used to measure the stiffness of the trap in situ. It also substantiates that there is no contact between the cell and the bead. As shown in Fig. 3, we chop up the signal for an interval, A of about 1 s to calculate the stiffness through the equipartition theorem [14]:

$$k = K_B \cdot T / var(z) \tag{4}$$

where *var(z)* is the variance of the *BD* (ΔZ in Eq. (1)) signal in interval A, K_B is the Boltzmann constant and T is the temperature of the medium. Since the stage velocity is very low ($\sim$1 μm/s), the Stokes drag force exerted on the bead during the PS movement is very small (<0.05 pN) and hence it can be neglected. In this setup, the trap stiffness can be varied from 5 to 30 pN/μm using powers of the trapping laser, at the sample, from 8 to 50 mW. Stronger stiffness can be obtained by increasing the power of the laser, but this is limited by the need to avoid damaging the cell. Note that cell damage is not only restricted to the induced death of the cell but also to alteration of its properties (e.g. mechanical properties). To exert sufficient care in this regards we kept the trap stiffness at a constant value: $k=15$ pN/μm (or 0.015 pN/nm, in units used by OT community), using a power of 24–26 mW of the trapping laser at the sample.

The interaction between the cell and the bead is observed for the second half of the sinusoid shown in Fig. 3. When the cell comes into contact with the bead and begins to push it, *BD* increases in the same direction as the PS travel. However, the rate of *BD* rise is smaller than the rate of PS displacement, PSD. The difference between the two gives the cell indentation, *Id*. As shown in Fig. 3, there are two characteristic regions for cell–bead interaction: indentation, when the stage/cell moves toward the

Please cite this article as: Yousafzai MS, et al. Substrate-dependent cell elasticity measured by optical tweezers indentation. Opt Laser Eng (2015), http://dx.doi.org/10.1016/j.optlaseng.2015.02.008

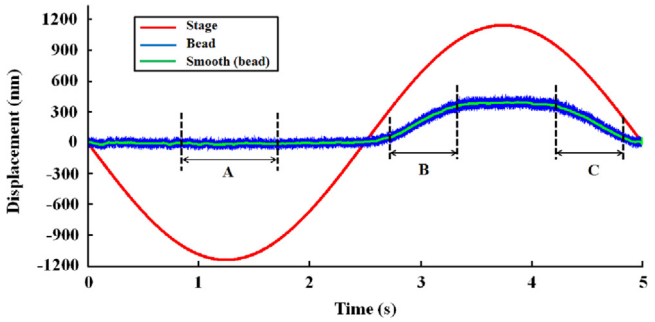

Fig. 3. Stage and bead displacement due to cell–bead interaction. Stage displacement following a period of sinusoidal signal ($T=5$ s) is represented in red. Bead displacement sampled at 10 kHz is represented by the blue curve and the corresponding smoothed signal (over 500 sampling points) by the green one. Trap stiffness is calculated using the signal chopped from interval A, where the bead is freely oscillating in the trap. Indentation, B and retraction, C intervals defined in the linear regions of the second half of the sinusoid are used to calculate the elastic modulus. (For interpretation of the references to colour in this figure legend, the reader is referred to the web version of this article).

bead and retraction, when the cell moves back. To measure the elastic modulus, we choose shorter intervals B (indentation) and C (retraction), corresponding to the almost linear regions of the stage movement. To avoid ambiguities related to the contact point, the starting point of the indentation interval should correspond to a bead displacement $BD > 30$ nm. The same condition is maintained for the second point of the retraction interval. Stage and bead displacements, indentation, the applied force and the selection of the indentation and retraction intervals are illustrated in Fig. 4. Details about the intervals length are given in next section.

2.3. Elastic modulus calculation

From the measurements of indentation and force the elastic modulus has been obtained by the use of the Hertz-model [28]. This model applies to homogeneous, semi infinite elastic solid objects, but a living cell is clearly different from that type of object, being viscous as well as elastic, and inhomogeneous. In spite of this, the Hertz-model has been used to determine cell elasticity in most reported cell mechanics studies [21,23,26–31] and technical procedures of commercial AFM instruments [34,35]. In fact, since the goal of most experiments is to make comparative studies between different cells or between cells under different environmental conditions, the use of Hertz-model can be justified. In our experiments, we consider the resulting elastic modulus as an *apparent* elastic modulus, to distinguish it from the rigorous formulation given by the Hertz-model. The *apparent* elastic modulus, E is given by [30]:

$$E = \left[3(1-\nu^2)/(4\sqrt{Id \cdot R})\right] \cdot (F/Id) \quad (5)$$

where, R is the bead radius, F the force, Id the indentation and ν is the Poisson ratio. For our experiments we choose $\nu = 0.4$ [30].

From the temporal sequences of BD and Id for the indentation and retraction intervals shown in Fig. 4, and using the force Eq. (3) we obtain the Force–indentation (F–Id) curves, shown in Fig. 5. As one can see from this figure, the curves are almost linear, indicating that the behavior of the cell at low indentation forces is elastic. By linearly fitting the Force–indentation (F–Id) curve we obtain a linear Force–Indentation (F_l–Id_l) curve (Fig. 5) of which slope S, is: $S = d(F_l)/d(Id_l)$. Considering this linear fit, the elastic modulus in Eq. (5) can be approximated by:

$$E = \left[3(1-\nu^2)/(4\sqrt{Id \cdot R})\right] \cdot S \quad (6)$$

with the indentation Id remaining the only variable. Since the absolute value of the indentation depends on a series of experimental variables, such as the contact point, it is difficult to determine it properly. To avoid this problem we have adopted a practical criterion, based on the observation of the experimental data. From the temporal sequences of the indentation curves (Fig. 4) we observed an indentation, $Id \geq 200$ nm, for all the cells analyzed in our study. The indentation and retraction intervals were therefore set to 200 nm. The starting point, t_1, of the indentation interval was always chosen to correspond to a bead displacement, $BD > 30$ nm, which confirms the cell–bead interaction event, while t_2 was chosen such that the interval $[t_1, t_2]$ remained within the linear region of the stage displacement and the indentation amplitude, measured from t_1, was higher than 200 nm. The same criterion was used to establish the retraction interval. Following the above considerations, we calculated the elastic modulus considering the same indentation value, $Id = 200$ nm, for all the cells in our study. Introducing this value and the radius of the bead ($R = 1.5$ μm) in Eq. (6) we obtain a simple equation to calculate the apparent elastic modulus:

$$E = 1150 \cdot S \quad (7)$$

where S is the slope of the linear force–indentation curve and the elastic modulus, E is expressed in [Pa].

3. Sample preparation for HBL-100 cells

HBL-100 is an immortalized human cell line, which was developed from the milk of a 27-year-old Caucasian woman with no evidence of breast cancer lesions [36]. Cells were

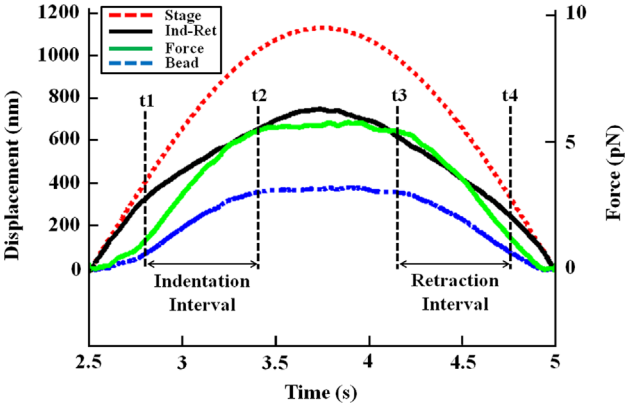

Fig. 4. Indentation and retraction intervals. Stage displacement (red), measured bead displacement (blue), the calculated force (green), calculated indentation (black) for the second half of the sinusoid, when cell interacts with the bead. Indentation and retraction intervals are selected in the linear regions of the sinusoid. (For interpretation of the references to colour in this figure legend, the reader is referred to the web version of this article).

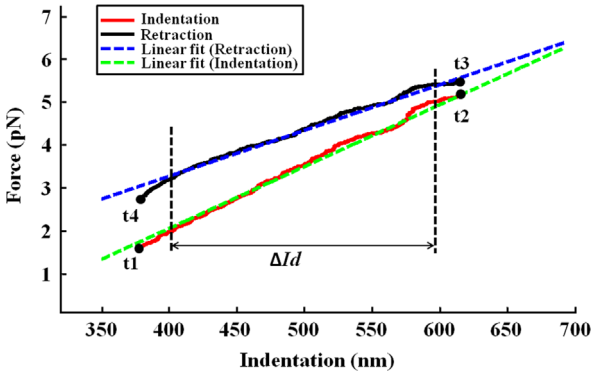

Fig. 5. Example of Force–Indentation plots taken for indentation and retraction intervals.

Please cite this article as: Yousafzai MS, et al. Substrate-dependent cell elasticity measured by optical tweezers indentation. Opt Laser Eng (2015), http://dx.doi.org/10.1016/j.optlaseng.2015.02.008

cultured in adhesion in a RPMI 1640 medium with stable L-glutamine (Euroclone), supplemented with 10% (v/v) fetal calf serum (FCS), and 50 IU/ml of Penicillin–streptomycin solution. Cell cultures were grown in 25 cm^2 flasks at 37 °C with 5% of CO_2. They were passed every 2–3 days, when they reached the confluence. The day before the experiment cells were detached from the flask using trypsin and seeded in 30 mm Petri dishes with a cover slip base at a density of 2×10^5 cells. They were maintained overnight in physiological conditions to let them adhere to the substrate. To test the influence of the substrate stiffness on the elastic modulus of the cell, the samples were seeded on bare and on collagen-coated Petri dishes. Type I Collagen at a concentration of 60 μg/ml in acetic acid 0.02 N was used for coating. The collagen was diluted at 60 μg/ml and distributed on a sterilized Petri dish to overlay the cover slip for 2 h under a laminar hood. The remaining solution was removed, air dried and put under UV light overnight.

4. Results and discussion

We investigated the validity of the experimental approach described in previous sections by measuring the elastic modulus of HBL-100 cells cultured on two different substrates: bare glass cover slip and collagen-coated cover slip. Since bare glass has a higher stiffness than collagen-coated glass [18,37]; we investigated whether this difference was reflected in the observations of the elastic modulus.

Here, an optically-trapped silica bead of 3 μm diameter was used as probe. The stiffness of the optical trap was kept constant (k=0.015 pN/nm) for all measurements. The stage was axially moved with a sinusoid signal (T=5 s, A=1.14 μm), allowing the measurement of the elastic modulus both for indentation and retraction at a loading rate of about 5 pN/s. We measured 26 cells cultured on bare substrates and 26 cells cultured on collagen coated substrates. For each substrate, the cells were selected from 10 different Petri dishes, from two different cultures. Measurements were performed for all cells in their central region, above the nucleus, as shown in Fig. 2c. Results are summarized in Fig. 6. HBL-100 cells cultured on glass had an elastic modulus higher than the one of the cells grown on collagen-I coated substrate, both for indentation (Ebi=26 ± 9 Pa, Eci=19 ± 7 Pa) and for retraction (Ebr=23 ± 10 Pa, Ecr=13 ± 7 Pa). The errors represent the standard deviations. For the glass (stiffer) substrate, the elastic modulus measured during indentation was 27% higher than that obtained for the more compliant collagen substrate. For retraction, the difference between glass and collagen-coated substrates was even larger: 43%. For both substrates, the elastic modulus measured for indentation was smaller than for retraction (by 11.5% for glass substrates and 31.6% for collagen-coated substrates).

The distribution of the elastic modulus values can be better observed from the box plot representation in Fig. 7. Notice that while the 50% clusters (2nd+3rd quartiles) are quite similar in dimension for all cases, the elastic modulus data for bare substrates have more spread than those for collagen coated substrates. A t-test has been applied to show the data sets are significantly different ($p < 0.01$).

Our results show that cell elasticity correlates with the substrate stiffness; HBL-100 cell elasticity increases when cells are cultured on stiffer substrate. Moreover, the elastic modulus

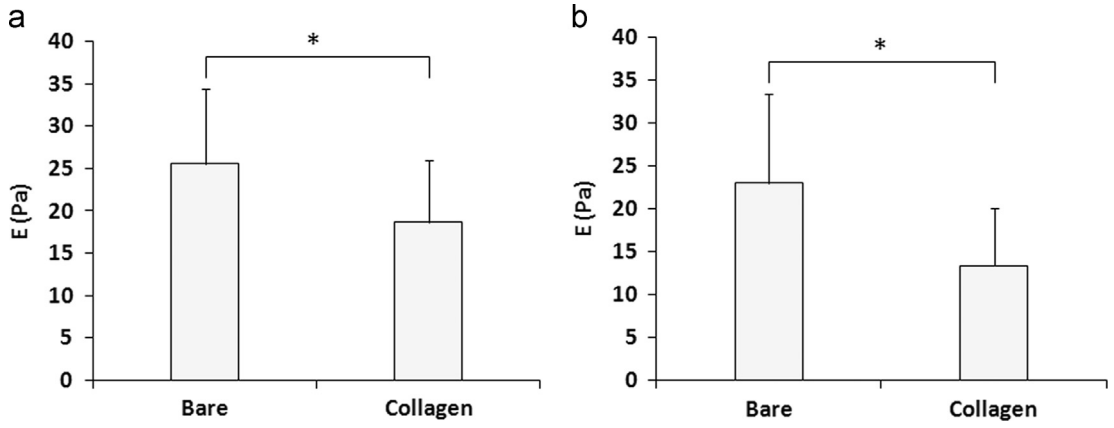

Fig. 6. Mean values of elastic modulus for (**a**) indentation and (**b**) retraction. (Nb, Nc=26; $p < 0.01$ (t-test)).

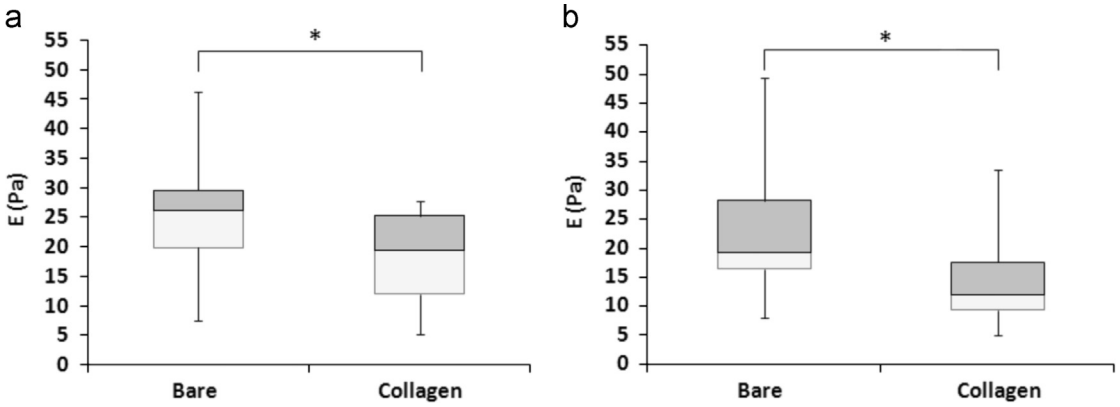

Fig. 7. Box plot representation of the distribution of elastic modulus for (**a**) indentation and (**b**) retraction. (Nb, Nc=26; $p < 0.01$ (t-test)).

Please cite this article as: Yousafzai MS, et al. Substrate-dependent cell elasticity measured by optical tweezers indentation. Opt Laser Eng (2015), http://dx.doi.org/10.1016/j.optlaseng.2015.02.008

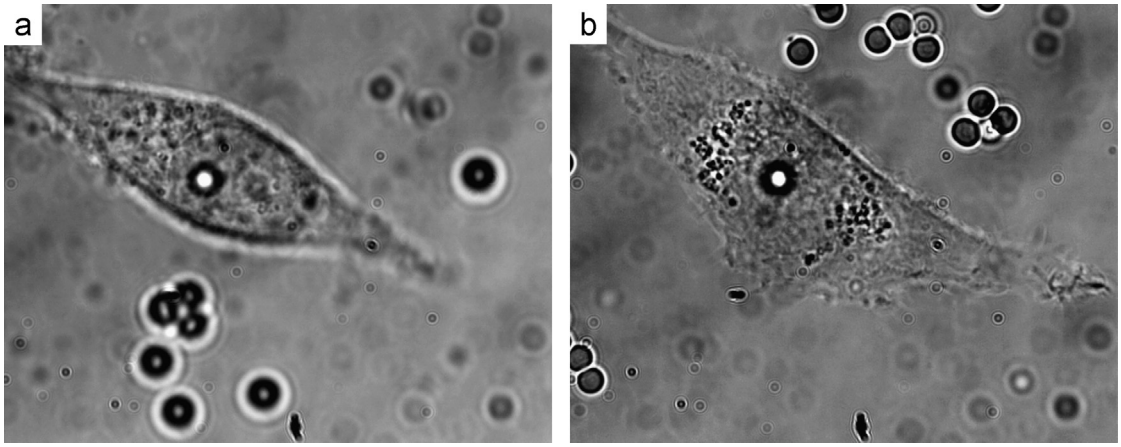

Fig. 8. Optical image of morphological changes of HBL-100 cells cultured on (**a**) collagen coated and (**b**) bare substrate.

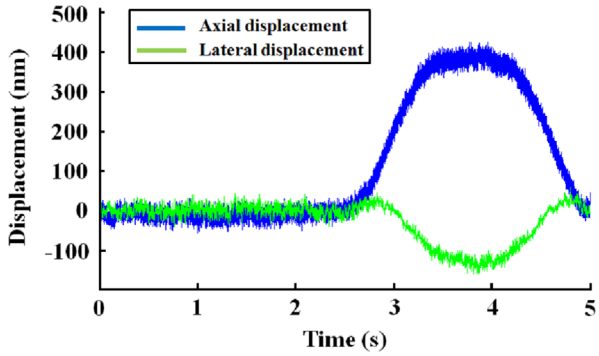

Fig. 9. Illustration of axial and lateral movement of the bead during cell–bead interaction.

probed at indentation is different from that measured during retraction. It is known that, for similar AFM cell elasticity measurements, the force–indentation curve at indentation is different from the retraction curve. The difference between those two curves has been explained by considering the energy dispersed by the cell between indentation and retraction, due to the viscous contribution [30]. Nevertheless, as shown by the force–indentation curve (Fig. 5), the cell–bead interaction is elastic and hence the viscous contribution can be discarded. Moreover, the difference between the two curves is opposite to that of AFM, meaning that more energy is spent at indentation than at retraction. It is not clear why this difference should exist. Since the interaction cell–bead takes place at a very low loading rate with respect to the AFM experiments, one reason might be a local reconfiguration of the plasma cell membrane (loose of elasticity) during indentation. This hypothesis will be checked in future experiments by applying different loading rates.

Substrate stiffness is known to influence the organization of cell cytoskeleton, showing that cells respond to extra-cellular environmental changes. Cytoskeleton re-arrangement is also accompanied by variations of cell spreading and motility. For instance, cells on compliant substrates exhibit reduced spreading, greater migration rates, and elevated lamellipodial activity compared with cells on more rigid substrates. Increased motility and lamellipodial activity on compliant substrates is associated with more dynamic focal adhesions, whereas cells on rigid substrates had more regularly shaped, stable adhesions [22,37,38]. Although the present study focuses on cell elasticity measurement and not on cell spreading and motility, the images acquired for each measured cell show that cells cultured on glass spread more than those cultured on collagen (see Fig. 8).

Besides the axial indentation, our setup allows us to monitor the lateral cell–bead interaction using BFP interferometry and the QPD sensor. This is a supplementary feature to the other two OT axial indentation setups reported in the literature [30,31]. Even if the displacement of the cell towards the bead is axial, the cell–bead interaction can induce a lateral displacement of the bead as well. This is due to the non-planar shape of the cell membrane in contact with the bead. An example of this, where we have tracked the bead in two directions, is shown in Fig. 9. The presence of a lateral component in the bead displacement implies that the indentation force is not perfectly vertical and the total force applied to the cell is bigger than the vertical indentation. Even if this lateral force is smaller than the vertical force, it is not negligible and it is important since it stresses the cell in a plane tangential to the surface membrane providing additional information about cell membrane elasticity and the mechanisms behind it. Monitoring the bead in more than one direction allows better evaluating the contact point and observing the cell–bead interaction. By using three dimensional (3D) tracking we plan to measure the 3D elasticity components and analyze in more detail the cell–bead interaction (e.g. slip, roll). Interestingly, working in scanning mode with feedback limited forces one can obtain the 3D local map of the cell topography from the 3D displacement of the bead. The topographic information, correlated with the elasticity map, will allow a more thoughtful characterization of the local 3D cell elasticity.

5. Conclusions

In this paper we demonstrated the strength of a simple optical tweezers setup to measure cell–bead interaction by axial displacement of the cell against a trapped bead. Force and elasticity measurements were performed at a low loading rate (5 pN/s) and with low forces (< 10 pN), thus providing a complementary regime to the AFM measurements, which are characterized by higher loading rates and forces. Cell elasticity was measured for HBL-100 cells cultured on two substrates with different stiffness, showing that cells adapt their elasticity to the compliance of the substrate: cells are observed to be less stiff with more compliant substrates. These results confirm that the substrate mechanical properties influence not only cell spreading and motility, but also cell elasticity.

Please cite this article as: Yousafzai MS, et al. Substrate-dependent cell elasticity measured by optical tweezers indentation. Opt Laser Eng (2015), http://dx.doi.org/10.1016/j.optlaseng.2015.02.008

Acknowledgments

We would like to gratefully acknowledge the Applied Physics section of the International Centre for Theoretical Physics (ICTP), Trieste for partial financial support to build the Optical Tweezers setup and partial financial support by the ERC Ideas Program through a senior Grant to GS, titled: MOlecular NAnotechnology for LIfe Science Applications: QUantitative Interactomics for Diagnostics, PROteomics and QUantitative Oncology (MONALISA QUIDPROQUO) Grant # 269051. FN acknowledges the ICTP-STEP program. We thank Daniela Cesselli from the University of Udine for critical reading of the manuscript and valuable suggestions.

References

[1] Ashkin A. Acceleration and trapping of particles by radiation pressure. Phys Rev Lett 1970;24:156.
[2] Ashkin A, Dziedzic J, Bjorkholm J, Chu S. Observation of a single-beam gradient force optical trap for dielectric particles. Opt Lett 1986;11:288–90.
[3] Grier DG. A revolution in optical manipulation. Nature 2003;424:810–6.
[4] Neuman KC, Block SM. Optical trapping. Rev Sci Instrum 2004;75:2787–809.
[5] Ashok PC, Dholakia K. Optical trapping for analytical biotechnology. Curr Opin Biotechnol 2012;23:16–21.
[6] Ashkin A, Dziedzic J. Optical trapping and manipulation of viruses and bacteria. Science 1987;235:1517–20.
[7] Ashkin A, Dziedzic J, Yamane T. Optical trapping and manipulation of single cells using infrared laser beams. Nature 1987;330:769–71.
[8] Ashkin A, Dziedzic J. Internal cell manipulation using infrared laser traps. Proc Natl Acad Sci 1989;86:7914–8.
[9] Block SM, Goldstein LS, Schnapp BJ. Bead movement by single kinesin molecules studied with optical tweezers. Nature 1990;348:348–52.
[10] Zhang H, Liu K-K. Optical tweezers for single cells. J R Soc Interface 2008;5:671–90.
[11] Ramser K, Hanstorp D. Optical manipulation for single-cell studies. J biophotonics 2010;3:187–206.
[12] Oddershede LB. Force probing of individual molecules inside the living cell is now a reality. Nat Chem Biol 2012;8:879–86.
[13] Moffitt JR, Chemla YR, Smith SB, Bustamante C. Recent advances in optical tweezers. Biochemistry 2008;77:205.
[14] Neuman KC, Nagy A. Single-molecule force spectroscopy: optical tweezers, magnetic tweezers and atomic force microscopy. Nat Methods 2008;5:491.
[15] Difato F, Pinato G, Cojoc D. Cell signaling experiments driven by optical manipulation. Int J Mol Sci 2013;14:8963–84.
[16] Huang H, Sylvan J, Jonas M, Barresi R, So PT, Campbell KP, et al. Cell stiffness and receptors: evidence for cytoskeletal subnetworks. Am J Physiol – Cell Physiol. 2005;288:C72–80.
[17] Schoen I, Pruitt BL, Vogel V. The Yin-yang of rigidity sensing: how forces and mechanical properties regulate the cellular response to materials. Annu. Rev. Mater. Res. 2013;43:589–618.
[18] Wen Q, Janmey PA. Effects of non-linearity on cell–ECM interactions. Exp. Cell Res. 2013;319:2481–9.
[19] Geiger TR, Peeper DS. Metastasis mechanisms. Biochim. Biophys. Acta (BBA)-Rev. Cancer 2009;1796:293–308.
[20] Makale M. Cellular mechanobiology and cancer metastasis. Birth Defects Res Part C: Embryo Today: Rev 2007;81:329–43.
[21] Guz N, Dokukin M, Kalaparthi V, Sokolov I. If cell mechanics can be described by elastic modulus: study of different models and probes used in indentation experiments. Biophys J 2014;107:564–75.
[22] Fischer RS, Myers KA, Gardel ML, Waterman CM. Stiffness-controlled three-dimensional extracellular matrices for high-resolution imaging of cell behavior. Nat Protoc 2012;7:2056–66.
[23] Mierke CT. The fundamental role of mechanical properties in the progression of cancer disease and inflammation. Rep Prog Phys 2014;77:076602.
[24] Tavano F, Bonin S, Pinato G, Stanta G, Cojoc D. Custom-built optical tweezers for locally probing the viscoelastic properties of cancer cells. Int J Optomechatronics 2011;5:234–48.
[25] Suresh S. Biomechanics and biophysics of cancer cells. Acta Mater 2007;55:3989–4014.
[26] Kirmizis D, Logothetidis S. Atomic force microscopy probing in the measurement of cell mechanics. Int J Nanomed. 2010;5:137.
[27] Laura Andolfi EB, Migliorini Elisa, Palma Anita, Pucer Anja, Skrap Miran, Scoles Giacinto, et al. Investigation of adhesion and mechanical properties of human glioma cells by single cell force spectroscopy and atomic force microscopy. (accepted). PloS one 2014.
[28] Li Q, Lee G, Ong C, Lim C. AFM indentation study of breast cancer cells. Biochem Biophys Res Commun 2008;374:609–13.
[29] Medalsy ID, Müller DJ. Nanomechanical properties of proteins and membranes depend on loading rate and electrostatic interactions. ACS nano 2013;7:2642–50.
[30] Nawaz S, Sánchez P, Bodensiek K, Li S, Simons M, Schaap IA. Cell viscoelasticity measured with AFM and optical trapping at sub-micrometer deformations. PloS one 2012;7:e45297.
[31] Dy M-C, Kanaya S, Sugiura T. Localized cell stiffness measurement using axial movement of an optically trapped microparticle. J Biomed Opt 2013;18:111411.
[32] MOTKwtc. ⟨https://www.thorlabs.com/NewGroupPage9.cfm?ObjectGroup_ID=3959⟩.
[33] Cojoc D, Cabrini S, Ferrari E, Malureanu R, Danailov MB, Di Fabrizio E. Dynamic multiple optical trapping by means of diffractive optical elements. Microelectron Eng 2004;73:927–32.
[34] JPK. ⟨http://www.jpk.com/atomic-force-microscopy.27.en.html⟩.
[35] BRUKER. ⟨http://wwwbrukercom/products/surface-analysis/atomic-force-microscopyhtml⟩.
[36] De Fromentel CC, Nardeux P, Soussi T, Lavialle C, Estrade S, Carloni G, et al. Epithelial HBL-100 cell line derived from milk of an apparently healthy woman harbours SV40 genetic information. Exp Cell Res 1985;160:83–94.
[37] Khademhosseini A, Borenstein J, Toner M, Takayama S. Micro and Nanoengineering of the Cell Microenvironment: Technologies and Applications. Norwood MA, USA: Artech House Publishers; 2008.
[38] Engler A, Bacakova L, Newman C, Hategan A, Griffin M, Discher D. Substrate compliance versus ligand density in cell on gel responses. Biophys J 2004;86:617–628.

Please cite this article as: Yousafzai MS, et al. Substrate-dependent cell elasticity measured by optical tweezers indentation. Opt Laser Eng (2015), http://dx.doi.org/10.1016/j.optlaseng.2015.02.008